

MODELLING AND SIMULATION OF DIFFUSION IN CHROMATOGRAPHIC RESIN USING SPATIALLY STRUCTURED RANDOM MEDIA AND A PARALLEL CELLULAR AUTOMATON

K. Nöh¹, M. Finke¹, W. Wiechert² and E. von Lieres¹

¹Research Centre Jülich, Institute of Biotechnology,
Leo Brandt Strasse, 52425 Jülich, Germany

²University of Siegen, Faculty of Mechanical Engineering
Am Eichenhang 50, 57068 Siegen, Germany

e.von.lieres@fz-juelich.de (Eric von Lieres)

Abstract

In liquid chromatography, effective diffusion coefficients are important parameters for the rational design of stationary phases and purification schemes. Common methods for the quantification of hindered diffusion in chromatographic media base on the analysis of dynamic data from experimental observations of protein migration. In contrast, stochastically driven approaches utilizing static data on matrix geometry and spatial hindrance structure allow studying this effect for arbitrary concentration profiles at the matrix boundary. A cellular automaton is implemented and applied for the analysis of hindered diffusion in spatially structured domains. A parallel 64 bit architecture enables calculation of large and densely populated automata. System states are stored in octrees in order to reduce both computing time and memory consumption. This automaton is used to quantify the deceleration of diffusion processes by different domain geometries, where obstacles are modeled by inaccessible cells. Random hindrance geometries are generated using clipped Gaussian fields that share macroscopic and microscopic properties with the chromatographic media, such as density, porosity and connectivity, which can be identified from measurement data. Although based on a stochastic characterization of random media, this simulation approach reveals information on the dynamics of chromatographic processes.

Keywords: Cellular automata, hindered diffusion, liquid chromatography, porous media, Gaussian fields.

Presenting Author's Biography

Katharina Nöh received her doctorate in Mathematics from Siegen University in 2006. In her thesis she generalized mathematical methods for the evaluation of metabolic flux experiments to non-stationary systems. She currently holds a position as post-doctoral researcher at the Research Centre Jülich, where she also applies high performance computing to various biotechnological systems.



1 Introduction

Liquid chromatography is a widely applied method for the separation of components of a mixture. Examples are found in biopharmaceutical industry where proteins are purified or in analytical chemistry [1]. Improved knowledge about the involved steps will lead to specially tailored design of separation processes. Thus, the cost and time consuming task of process optimization for new products can be reduced.

In-depth understanding of the overall process includes two different aspects. First, knowledge of the (mean) residence times of molecules on the surface of adsorbers, which results in the interaction of the solute molecules with the so called stationary phase [2]: Various models exist modeling these interactions and it is a current challenge to refine existing modeling, simulation and experimental approaches with the aim of quantitative prediction of biomolecule separation [3].

The second aspect is the transport of solutes and the associated peak widening of different species through the chromatographic column due to diffusion and dispersion. However, experimental investigation of these micro-dynamic processes is difficult because this requires time-dissolved observation of peaks of a tracer solute in a cross-section of the material under investigation [1]. Recently, the use of fluorescence labels provides additional insight into transport phenomena in chromatographic media [4]. Digital image analysis and reconstruction methods are developed accordingly [5].

Stationary phases and, consequently, purification schemes are characterized by the diffusion coefficients of the separated proteins in the media. In particular, the actual porous structure influences the intra-particle diffusion. A recent experimental approach for the determination of intra-particle protein diffusion coefficients is based on the analysis of measured concentration profiles [6]. This study is now complemented by an approach for the prediction of diffusion phenomena on the basis of directly observable properties of the inner particle geometry instead of rather indirect observations of intra-particle concentration profiles.

Computer simulations in the interior of a spatially structured particle (cf. Figure 1) are applied for the estimation of the influence of spatial obstacles on the diffusion process. The porous structure can be characterized by directly available stereological characteristics, such as porosity, pore size distribution, pore scale and orientation. A stochastic-based algorithm is used to quantify the deceleration of diffusion processes in comparison with free diffusion. The adsorption and desorption of molecules at the pore walls can be potentially included in this approach.

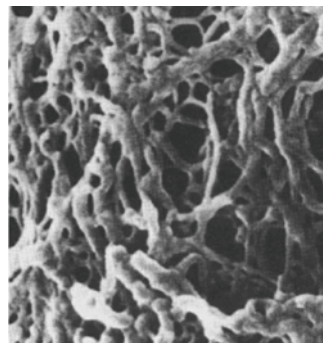


Fig. 1 Three dimensional structure of a chromatographic resin (2 % agarose gel) [7].

2 Cellular Automata

Cellular automata (CA) were originally introduced by von Neumann and Ulan in the 1950s and provide a powerful instrument for modeling and investigating the behavior of continuous physical systems. In recent years, CA have become popular for the simulation of spatio-temporal processes, as alternative to complex partial differential equations. Usually, CA are systems in which time and space are discrete quantities. Their essential properties are:

- A regular n -dimensional lattice ($n=1,2,3$ in practice). Each cell of this lattice is in one of a finite number of possible discrete elementary states.
- A dynamic behavior that is specified by identical transition rules for synchronous updating of all cell states in the lattice in each time step. These cellular transition rules depend on the choice of an interaction neighborhood, i.e., the new state of a cell is determined on the basis of the previous states of specific surrounding cells. Such simple rules allow modeling of rather complex behavior.
- A specification of the initial configuration, i.e. a snapshot of all cell states at $t = t_0$ and a set of boundary conditions are required. Spatial periodic boundary conditions can be used to approximate infinite lattices.

The implemented CA for the simulation and analysis of hindered diffusion processes bases on the three dimensional update rules introduced by Chopard and Droz [8]. In this CA, cubic cells are occupied by up to six diffusing particles. Hence, the number of occupants never exceeds the number of adjacent cells with shared faces. In order to avoid overfilling, the faces must not be crossed by more than one particle in each direction in any time step. The update process transfers all particles to adjacent cells, following combinatorial probability rules. The actually applied automaton is realized by six basic cellular update

patterns, namely ballistic trajectory, four symmetric and randomly chosen deflexions and a reflexion, as illustrated in Figure 2. This realization provides a limited complexity of the possible transition rules. The simulated diffusion processes are characterized by the probabilities of ballistic trajectory and reflexion, as well as the spatial and temporal discretization.

$$D \approx \frac{\Delta x^2}{\Delta t} \cdot \frac{1}{6} \cdot \frac{1 + p_b - p_r}{1 - p_b + p_r} \quad (1)$$

Here, D is the diffusion coefficient and Δx and Δt specify the discretization in space and time respectively. The four deflexion probabilities p_d are equal, due to symmetry, and determined by $p_b + 4 \cdot p_d + p_r = 1$, since one of the patterns must always be chosen. Probabilities of adjacent cells are assumed independent of each other.

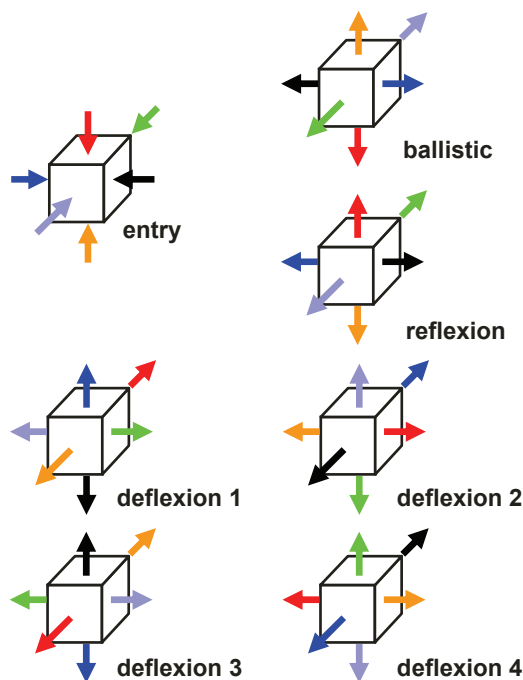


Fig. 2 The update process is described by six probabilistic update rules.

A modeling approach with discrete spatial data has been chosen in order to describe hindered diffusion processes that are governed by micro-structural characteristics of the medium. Obstacles need to be generated according to material constants that are determined from measurement data. The knowledge of the media is typically much less detailed than required for deterministic prediction of transport processes, however, random fields provide a natural description of resin heterogeneities. The obstacles are thus

generated using discrete random fields and implemented as inaccessible cells, described in more detail in the following section.

The implemented CA is used to quantify the deceleration of diffusion processes resulting from different domain geometries. Hindered diffusion coefficients are estimated from the simulation results by comparison with free diffusion.

$$\frac{\partial c}{\partial t}(x, t) = D \cdot \frac{\partial^2 c}{\partial x^2}(x, t) \quad (2)$$

Here, c denotes the concentrations at position x and time t . Analytic solutions are known for particular domains, for instance the Cartesian half space given by $x \geq 0$, initial concentration $c(0, x) = 0$ and constant boundary concentration $c(t, 0) = c_0$ (erf is the error function).

$$c(x, t) = \frac{c_0}{2} \cdot \left(1 - erf \left(\frac{x}{2 \cdot \sqrt{D \cdot t}} \right) \right) \quad (3)$$

3 Gaussian Random Fields

Poisson densification processes are straightforward models for the generation of irregular spatial structures: Regularly shaped particles, such as spheroids and rectangular bars, are placed in a spatial region, one after the other in an independent random process following physical particle characteristics. This approach is conceptually rather simple but well understood. Physical properties, for instance the volume fraction of pore walls, are easy to incorporate [9]. Porous media used in liquid chromatography are, however, structurally more complex (see Figure 1 for a typical example) and, thus, require more realistic modeling.

Joshi, Quiblier and Adler present an approach for the statistical reconstruction of random porous media, basing on the first two moments, namely the porosity and an auto-correlation function, which are determined by morphologic qualities [10-12]. This method can be supplemented by further information on structural and geometric properties of the micro-structures. Moreover, this approach allows generation of disordered media with the desired properties in silico.

We successfully apply simulative methods that are based on level-cuts through correlated Gaussian fields that are superpositions of random plane waves and were originally described for phase separations from single phase fluids [13,14]: Discrete random fields are obtained by clipping a stationary mean Gaussian random field at one or several fixed thresholds. The model is parameterized by the family of underlying covariance functions for the Gaussian field, the chosen

set of levels, and a vector specifying particular covariance parameters.

3.1 Basic Definitions

A collection of random variables that are indexed over a set is called a *stochastic process*.

$$\{X(\mathbf{x}, t) : (\mathbf{x}, t) \in I \times \mathbb{R}^+ \subset \mathbb{R}^d \times \mathbb{R}^+\} \quad (4)$$

Due to the Daniel-Kolmogorov theorem it is sufficient to consistently specify the joint distribution of any finite subset $\{X(\mathbf{x}_1, t), X(\mathbf{x}_2, t), \dots, X(\mathbf{x}_n, t)\}$, thus for $\mathbf{y} \neq \mathbf{x}_1, \mathbf{x}_2, \dots, \mathbf{x}_m$ the underlying probability measure fulfills $P(X(\mathbf{x}_i, t), i = 1, \dots, m, X(\mathbf{y}, t)) = P(X(\mathbf{x}_i, t), i = 1, \dots, m)$. For any stochastic process that contains a spatial variable \mathbf{x} , the set (4) is called *random field*. A random field is *stationary* if its distribution remains invariant under translations of the index set I . For convenience the parameter t is neglected in the following.

A random vector $\mathbf{x} = (\mathbf{x}_1, \mathbf{x}_2, \dots, \mathbf{x}_n)^T$ is *multivariate normal* if each linear combination of random variables is still normally distributed. A random field $X(\mathbf{x})$ is a *Gaussian random field* if $X(\mathbf{x}_1), X(\mathbf{x}_2), \dots, X(\mathbf{x}_m)$ is multivariate normal for any $\mathbf{x}_i \in I$. For each random field the *mean function* $\boldsymbol{\mu}(\mathbf{x})$ and the *covariance function* $\boldsymbol{\rho}(\mathbf{x}_1, \mathbf{x}_2)$ are defined.

$$\boldsymbol{\mu}(\mathbf{x}) = E[X(\mathbf{x})] \quad (5)$$

$$\boldsymbol{\rho}(\mathbf{x}_1, \mathbf{x}_2) = \text{Cov}(X(\mathbf{x}_1), X(\mathbf{x}_2)) \quad (6)$$

The corresponding probability density can be written as:

$$f_x(\mathbf{x}) = \frac{1}{\sqrt{(2\pi)^d \boldsymbol{\rho}}} \exp\left(-\frac{1}{2}(\mathbf{x} - \boldsymbol{\mu}) \cdot \boldsymbol{\rho}^{-1} \cdot (\mathbf{x} - \boldsymbol{\mu})^T\right). \quad (7)$$

$X(\mathbf{x})$ is a *mean zero* Gaussian field if the expectation value fulfills $E[X(\mathbf{x})] = \mathbf{0} \quad \forall x$. The covariance of a zero mean field is then given by $\boldsymbol{\rho}(\mathbf{x}_1, \mathbf{x}_2) = E[X(\mathbf{x}_1) \cdot X(\mathbf{x}_2)]$. Two fields X_1 and X_2 are *independent* if $X_1(\mathbf{x}_1)$ and $X_2(\mathbf{x}_2)$ are independent for any $\mathbf{x}_i \in I$. More formal definitions are given in [15].

Gaussian processes have the advantage that the field distributions are completely determined by their mean and covariance functions (5) and (6). Any function

$\boldsymbol{\mu}(\mathbf{x})$ can be the mean function of a Gaussian field, whereas symmetry and non-negative definiteness are necessary and sufficient conditions on $\boldsymbol{\rho}(\mathbf{x}_1, \mathbf{x}_2)$ [16]. In this contribution, stationary Gaussian fields with constant mean $\boldsymbol{\mu}(\mathbf{x}) \equiv \boldsymbol{\mu}$ are used for modeling random media. Hence, $\boldsymbol{\rho}(\mathbf{x}_1, \mathbf{x}_2)$ is only a function of the difference $\mathbf{x}_1 - \mathbf{x}_2$.

3.2 Generation of Gaussian Fields

Assuming stationarity, realizations of Gaussian fields are available that are based on spectral methods [14]. It is well known, that Gaussian fields with periodic boundaries can be calculated as finite sums over cosine series whose coefficients have uniformly distributed wavelength and amplitudes that are proportional to the spectral density function of the process. Practically, the power spectrum of a correlated field (see Table 1 for examples) is determined via Fast Fourier Transform (FFT). A field of independent normally distributed random numbers is generated and convoluted linearly. In this way it is transformed into the spectral domain where the corresponding phase spectrum is evaluated (*linear filtering*, [11]). In a second step, the correlated field is generated with the random phase spectrum and the power spectrum as required components for the inverse FFT back into spatial Cartesian coordinates. A threshold cut is performed such that the statistical properties of the generated field agree with preset values (*nonlinear filtering*, [11]). An alternative approach originally proposed in [17] includes two-level thresholding of the correlated Gaussian field, which defines a volume between two isosurfaces.

Tab. 1 Correlation function families

ζ	$\mathbf{R}(\Delta\mathbf{x}, \lambda, \beta, \zeta)$
1: exponential	$\exp(- \Delta\mathbf{x} /\lambda)^\beta$
2: stable	$\exp(-\sqrt{ \Delta\mathbf{x} /\lambda})^\beta$
3: Gaussian	$\exp(-(\Delta\mathbf{x}/\lambda)^2)^\beta$
4: power	$(1+ \Delta\mathbf{x} /\lambda)^{-\beta}$
5: spherical	$1 + 3 \cdot \Delta\mathbf{x} /(2 \cdot \lambda) + (\Delta\mathbf{x} /\lambda)^3/2,$ $ \Delta\mathbf{x} \leq \lambda$

Typical correlation function families $\mathbf{R}(\Delta\mathbf{x}, \lambda, \beta, \zeta)$ with $\Delta\mathbf{x} = \mathbf{x}_1 - \mathbf{x}_2$ and scaling parameters $\lambda > 0, \beta$, that are commonly used and implemented, are given in Table 1. An additional scaling parameter $\beta \in \mathbb{R}$ is added in order to improve flexibility.

All functions $\mathbf{R}(\Delta\mathbf{x}, \lambda, \beta, \zeta)$ decay asymptotically as the ratio $\Delta\mathbf{x}/\lambda$ tends towards infinity. However, they differ substantially in their form as is shown in Figure 3.

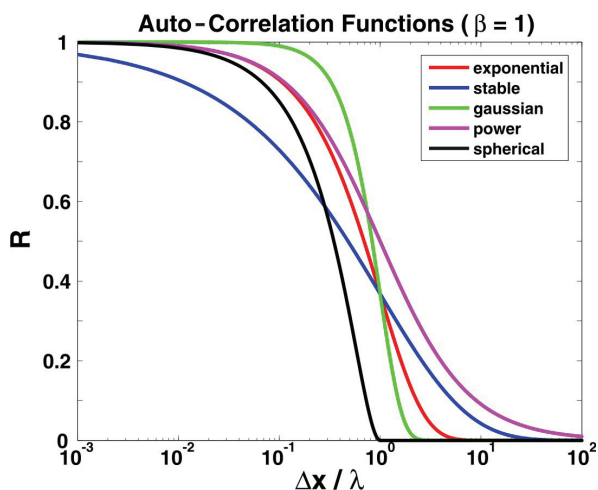


Fig. 3 Correlation functions $\mathbf{R}(\Delta\mathbf{x}, \lambda, 1, \zeta)$ (see Table 1). The x-axis is logarithmically scaled.

Applying the reconstruction method of Adler, the first two geometric characteristics, i.e. the porosity Φ (1st spatial moment) and the auto-correlation function (2nd spatial moment) are available. The realization of these two moments is parameterized in our model by the parameter set

$$\theta = (\zeta, \mu, \sigma, \lambda, \varphi^T, \alpha^T, \beta, L)^T \quad (9)$$

with

- $\zeta \in \{1, 2, 3, 4, 5\}$, the type of model family as shown in Table 1
- $\mu, \sigma, \lambda > 0$, the mean, variance and correlation length, respectively, of the Gaussian random process, as determined by the first two spatial moments.
- φ , the rotation angles for Gaussian field (gyratory degrees of freedom)
- Level-cuts:
 - $\alpha \in \mathbb{R} : \alpha \leq x$ single-cut thresholding

- $\alpha_1, \alpha_2 \in \mathbb{R} : \alpha_1 \leq x \leq \alpha_2$ two-cut thresholding

The single cut can be recovered from the two-cut approach by setting $\beta = \infty$.

- $\beta \in \mathbb{R}$, a scaling factor
- $L > 0$, the grid size

The set $\theta = (3, 0, 1, 1, (0,0,0), 0.4, 1, 512)^T$ is used, unless otherwise specified.

3.3 Typical Results

A large variety of micro-structured textures can be created by choosing different covariance functions \mathbf{R} and thresholds α , for example to reach a predefined volume fraction [18]. Some examples are given in Figure 4. The random fields with correlation functions $\zeta \in \{2, 4\}$ exhibit rather similar characteristics when compared to the case $\zeta = 1$ (exponential).

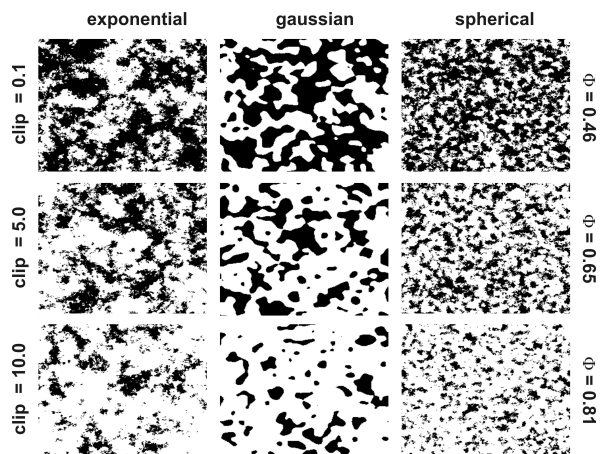


Fig. 4 Cross-sections through three-dimensional models of porous media with different correlation functions (see Table 1) and clipping thresholds α . The images are generated on a $512 \times 512 \times 512$ voxel grid, and accessible pores are shown in white.

Figure 5 shows pore structures that are derived from Gaussian random fields with different thresholds. The granularity of the disordered material is effectively controlled by the correlation length λ of the correlation function \mathbf{R} .

Random fields in three spatial dimensions generated for an area of $256 \times 256 \times 256$ voxels on the basis of Gaussian random fields with a fixed covariance function but different variances σ are presented in Figure 6. The clipping levels are chosen such as to maintain a constant porosity.

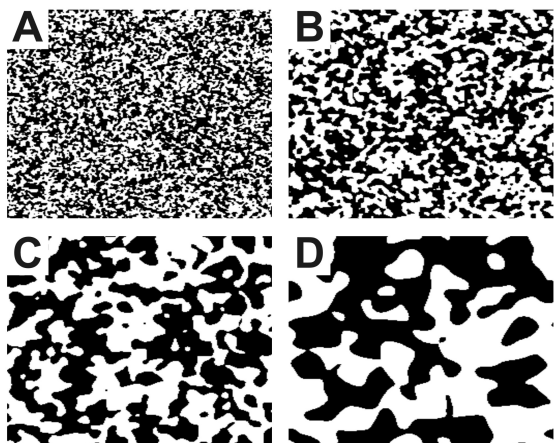


Fig. 5 Binary-phase images of Gaussian random fields for different correlation lengths $\lambda = 2^i, i = 1, 2, 3, 4$ (A, B, C, D). A fixed clipping threshold of $\alpha = 0.8$ is chosen such as to maintain a porosity of $\Phi = 0.49$.

The voxel model has the grid size $L = 512$ and accessible pores are shown in white.

Two-cut thresholding models exhibit a ribbon-like structure (data not shown). Hence, realizations with high interconnectivity are possible even for high porosities. Moreover, the concept of level-cut models can be generalized to incorporate more than two thresholds.

4 CA Implementation

For the quantification of system properties, CA simulations are performed on large lattices. Cubes of 1024^3 to 4096^3 voxels are used in order to avoid boundary effects. Analyses of many realizations of the hindrance structures reduce the impact of the stochastic generation algorithm. Obstacles are only generated on sub-cubes of the total CA space, for instance with $L = 256$. Periodic structure generation allows homogeneous filling of the total space with disordered obstacles.

CA are ideally suited for parallel computing, owing to a close correspondence to SIMD hardware. The computational time is significantly reduced by partitioning the spatial domain into cuboids. A versatile implementation of the CA using MPI communication standards is maintained for both 32 bit and 64 bit architectures. This allows allocation of 1024^3 or more than 2000000^3 cells, respectively. The CA is implemented in C++ and follows a strict object-oriented design. More implementation details are presented in [19].

The underlying lattice contains four different cell types: interior cells, obstacles, boundary, and source cells. In order to enable fast access and efficient storage of the three dimensional data, system states as

well as obstacle, boundary and source coordinates are stored in separate octrees (Figure 8). The current CA implementation is designed for static obstacles that are generated during the initialization of the simulation process. The inaccessible cells are first marked in a temporary Cartesian structure which is subsequently traversed and translated to an obstacle octree. In the cell occupancy tree of the interior system states those cell faces are marked, that are adjacent to inaccessible obstacle cells, as illustrated in Figure 7.

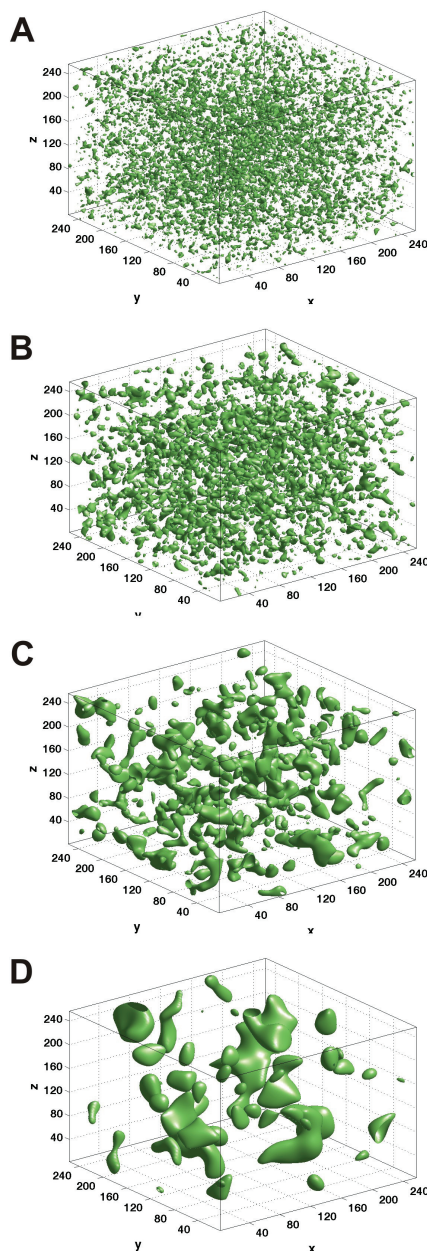


Fig. 6 Three dimensional interfaces of sample random fields that are generated on the basis of a Gaussian random field with fixed covariance function. For the different variances σ (A: 3, B: 5, C: 10, D: 20), the corresponding clipping levels α are determined such as to maintain a constant porosity Φ of 10 %.

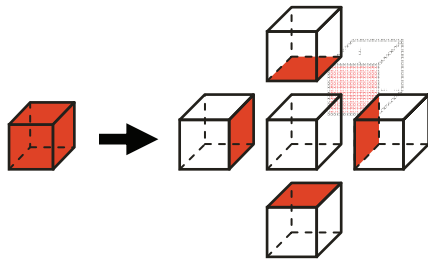


Fig. 7 Inaccessible obstacle cells are implemented as impermeable faces of the adjacent cells. (The front cube is omitted.)

The storage of impermeable faces instead of inaccessible cells improves obstacle testing, since diffusing particles and interfered obstacles share the same octal coordinates. In contrast to the invariant obstacle tree, the octree for the system states is traversed in each update step and discarded after the updated occupancies are stored in a new tree. The source cells are randomly filled with a predefined density that can be chosen as a function of time. In order to maintain this specified density, the source cells need to be randomly replenished or thinned out previous to each update step. A data structure for the domain boundaries is required for the handling of particles which diffuse between domains and that are, hence, processed on different nodes.

4.1 Typical Results

All simulations were performed in Jülich on the super-computer JUMP. The obstacles are generated on 512^3 voxels with a correlation function of Gaussian type, correlation length 10 and clipping levels 0.30 and 0.35. The resulting three-dimensional hindrance structures are similar to that in Figure 6c. The obstacle storage in Cartesian coordinates costs approximately 4 megabytes.

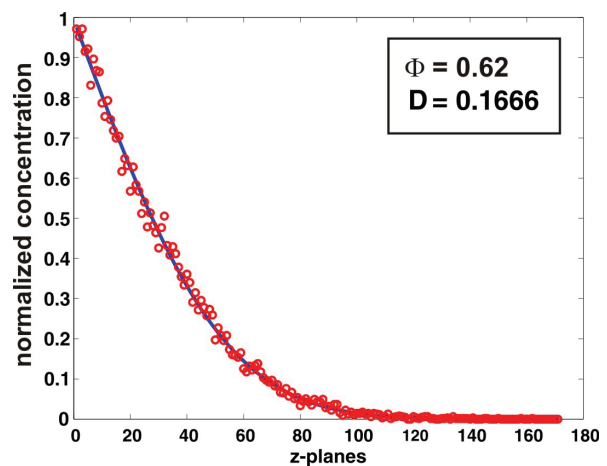
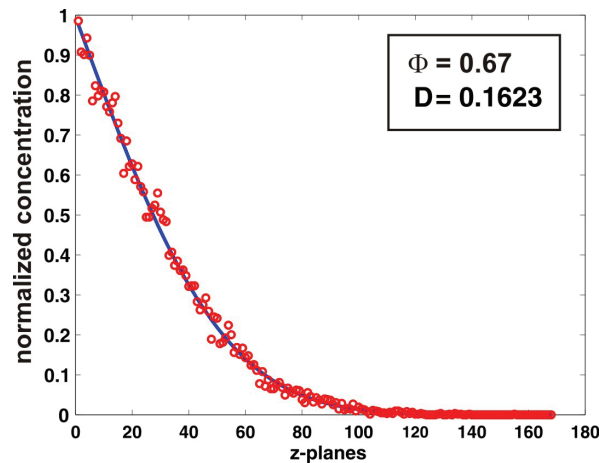


Fig. 9 Projections of CA fillings on the z-axis after 5000 time steps (red), and analytical solution of the equation for free diffusion with the effective diffusion coefficient (blue).

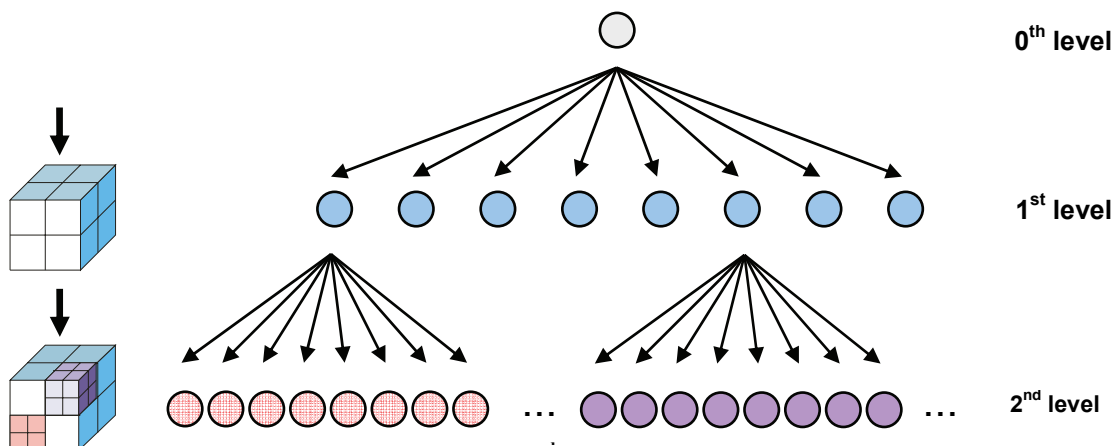


Fig. 8 Octrees represent spaces that are occupied by a juxtaposition of cubes where sizes and positions are powers of 2, and index a recursive decomposition of these spaces. This makes the octree structure ideal for efficient storage and fast access of three-dimensional data for densely populated CA.

At the upper boundary of the CA, a constant density of diffusing molecules is maintained at all times, whereas the lower boundary is left open. The left and right side, as well as the front and back are connected by periodic boundary conditions, respectively. An empty automaton is chosen as initial condition.

This setup is applied for the simulation of 5000 time steps of the hindered diffusion process. The resulting CA fillings are projected on the z-axis, as shown in Figure 9. The analytical solution of the corresponding equation for free diffusion (Equation 3) is fitted to this data in order to determine the effective diffusion coefficient in the investigated media.

5 Outlook

Computer tomography combined with two- and three-dimensional image analysis will help to gain further insight into the micro-structures of chromatographic resin. Their physical properties can be determined from high quality volume images. On the basis of discrete images, the clipping levels of correlated Gaussian fields can be estimated by comparing the observed area functions with the moments of the normal distribution. The various model parameters that are listed in Section 3.2 can be estimated for any suitable family of underlying covariance functions \mathbf{R} of the Gaussian field. Random fields that share specific characteristics with real media can be used to generate new images. These are qualitatively compared with the original images in order to evaluate how realistic the artificial obstacles are.

Voronoi tessellation provides an alternative concept for modeling random media, especially for foam-like structures [20]. Here the seed of an initially chosen kernel is propagated in fiber-like structures to space covering cells. The Gaussian approach that is presented in this contribution will be compared to the Voronoi approach in a future study.

Not only metric but also topological properties, such as structural pore interconnectivity, surface area and curvature are important characteristics of porous media [21]. Here, Minkowsky functionals are promising in that they determine not only the connectivity but also the shape of spatial binary figures [22].

6 References

- [1] H. Schmidt-Traub. Preparative Chromatography of Fine Chemicals and Pharmaceutical Agents. Wiley-VCH, Weinheim, 2005.
- [2] D. M. Ruthven. Principles of Adsorption and Adsorption Processes. John Wiley & Sons Inc, New York, 1984.
- [3] G. Guiochon, A. Felinger, D. G. Shirazi, and A. M. Katti. Fundamentals of Preparative and Nonlinear Chromatography. Academic Press Inc., U.S., 2006.
- [4] J. Hubbuch, T. Linden, E. Knieps, A. Ljunglöf, J. Thömmes, and M.-R. Kula. Mechanism and Kinetics of Protein Transport in Chromatographic Media studied by Confocal Laser Scanning Microscopy Part I+II. *Journal of Chromatography A*, 1021, 93–104 and 105–115, 2003.
- [5] C. Niehoff. Particle Tracing and Robust Mean Value Estimation from Confocal Laser Scanning Microscopy Data (in German), University of Applied Sciences Aachen at Jülich, 2006.
- [6] M. Schröder, E. von Lieres, and J. Hubbuch. Direct Quantification of Intraparticle Protein Diffusion in Chromatographic Media, *Journal of Physical Chemistry B*, 10(3):1429-1436, 2006.
- [7] J.-C. Janson, and L. Rydén (Editors). Protein Purification: Principles, High Resolution, Methods, and Applications, Wiley – VCH, Weinheim, 1998.
- [8] B. Chopard, and M. Droz. Cellular Automata Modeling of Physical Systems, Cambridge University Press, Cambridge, 1998.
- [9] J. B. Keller. Conductivity of a medium containing a dense array of perfectly conducting spheres of cylinders or nonconducting cylinders. *Journal of Applied Physics*, 34:991-993, 1963.
- [10] M. Joshi. A Class of Stochastic Models for Porous Materials. Ph. D. thesis, University of Kansas, Lawrence, 1974.
- [11] J. A. Quiblier. A new three-dimensional modelling technique for studying porous media. *Journal of Colloid Science*, 98: 84-102, 1984.
- [12] P. M. Adler. Porous Media: Geometry and Transports. Butterworth/Heinemann, 1992.
- [13] N. F. Berk. Scattering Properties of the Level-set Model of Random Morphologies. *Physical Review A*, 44:5069-5079, 1991.
- [14] M. Teubner. Level Surfaces of Gaussian Random Fields and Microemulsions, *Europhysics Letters*, 14:403-408, 1991.
- [15] R. J. Adler. The Geometry of Random Fields, John Wiley & Sons Inc, New York, 1981.
- [16] D. M. Bates and D. G. Watts. Nonlinear Regression Analysis and its Applications. John Wiley & Sons Inc, New York, 2007.
- [17] J. W. Cahn. Phase Separation by Spinodal Decomposition in Isotropic Systems. *Journal of Chemical Physics*, 42:93-99, 1965.
- [18] A. P. Roberts, and M. Knackstedt. Structure-Property Correlations in Model Composite Materials. *Physical Review E*, 51: 4141-4154, 1995.

- [19] E. von Lieres, M. Finke, and U. Buschmann. Simulation of Hindered Diffusion in Spatially Structured Domains Using a Parallel Cellular Automaton, In I. Troch and F. Breiteneker, editors, 5. Vienna International Conference on Mathematical Modelling, Vienna, 2006, Argesim.
- [20] C. Monnereau and M. Vignes-Adler. Optical Tomography of Real Three-dimensional Foams. *Journal of Colloid and Interface Science*, 202:45-53, 1998.
- [21] Z. Liang, M. A. Ioannidis, and I. Chatzis. Geometric and Topological Analysis of Three-Dimensional Porous Media: Pore Space Partitioning Based on Morphological Skeletonization, *Journal of Colloid and Interface Science*, 221:13-24, 2000.
- [22] K. R. Mecke and D. Stoyan, (Editors). *Statistical Physics – The Art of Analyzing and Modeling Spatial Structures*. *Lecture Notes in Physics*, Volume 554, Springer, Berlin, 2000.